Available online at www.sciencedirect.com
SCIENCE DIRECT®
International Journal of Heat and Mass Transfer 48 (2005) 4623–4632
International Journal of HEAT and MASS TRANSFER
www.elsevier.com/locate/ijhmt

Experimental and numerical investigation of gaseous fuel combustion in swirl chamber

Stevan Nemoda *, Vukman Bakić, Simeon Oka, Goran Zivković, Nenad Crnomarković

Laboratory for Thermal and Energy Research, "Vinča" Institute of Nuclear Sciences, P.O. Box 522, 11000 Belgrade, Serbia and Montenegro

Received 22 November 2004
Available online 14 July 2005

Abstract

In this paper the results of experimental and numerical investigations of swirl burner were presented. Mathematical model for prediction of velocity, temperature and concentration fields of axisymmetrical confined swirl turbulent flame was developed. Model consists of few mutually coupled segments related to basic processes in turbulent flows with combustion. The original combustion rate model based on the ideal reacting hypothesis within fine structure of turbulence was applied. The comparison of the experimental results with computation showed satisfactorily agreement between the model and the experiment. This analysis also showed the importance of the proposed combustion rate model with simultaneous influence of both chemical kinetics and turbulent effects.

Keywords: Swirling burner; Swirl flow; Turbulence; Combustion; LDA measurements

1. Introduction

Swirl flows are widely used in various technical devices and technological processes especially in the reacting flow, where the existence of recirculation zones leads into the increase of efficiency of chemical reaction and stabilization of processes. Due to the permanent increase in the development of these devices, experimental investigation and mathematical modeling of swirl turbulent flow are very important.

For the purpose of computer simulation of gaseous fuel burners and combustion chambers a mathematical model and numerical solution procedure, for the prediction of the turbulent swirl flow with heat and mass transfer for combustion in two-dimensional geometries: plane and axisymmetrical was developed. In this work the model was applied to the analysis of swirl combustion chamber.

The problems of flow and heat transfer in boiler furnaces and combustors are of a complex nature, and hence attention must be focused on the general principles which govern the behavior of the flow in such complex configurations. According to this the mathematical model of processes in the combustion chamber consists of four basic segments: turbulent swirl flow, convective heat and mass transfer, chemical reactions, radiative heat transfer.

For validation of the results of mathematical modeling two experimental apparatus were completed: for the

* Corresponding author.

0017-9310/$ - see front matter © 2005 Elsevier Ltd. All rights reserved.
doi:10.1016/j.ijheatmasstransfer.2005.04.004

Nomenclature

A	constant in algebraic expression for turbulent dissipation rate [–]
a_γ, a_τ	constants of combustion rate model [–]
C_μ	constant in effective viscosity expression [–]
c_p	specific heat [J kg^{-1} K^{-1}]
E_a	energy of activation [J mol^{-1}]
K_a	absorption coefficient [m^{-1}]
k	kinetic energy of turbulence [J kg^{-1}]
M_k	molecular mass of species k [kg mol^{-1}]
ℓ	macro-scale length of turbulence [m]
m_k	mass fraction of species k [–]
n_k	stoichiometric molecule number of species k [–]
q_w	heat flux on a wall [W m^{-2}]
R	universal gas constant [J mol^{-1} K^{-1}]
R_k	conversion rate of species k [kg m^{-3} s^{-1}]
r, x	radial and axial coordinate [–]
S	swirl number [–]
S_R	radiation source term [W m^{-3}]
T	temperature [K]
u	root of the mean-square velocity fluctuations [m s^{-1}]
u, v, w	fluctuating component of the axial, radial and tangential velocity respectively [m s^{-1}]

Greek symbols

ε	turbulence dissipation rate [m^2 s^{-3}]
μ	viscosity [Pa s]
ρ	density [kg m^{-3}]
τ^*	time micro-scale [s]

Subscripts

fu	fuel
k	chemical species
ox	oxygen

Superscripts

$'$	fluctuations
$*$	fine structures
$\circ$	surrounding fluid

measurements of instantaneous velocities within isotherm swirl chamber using laser Doppler anemometry (for the validation of the turbulent model), and for the measurements of the temperature field using thermocouple and concentrations of species of combustion products in the swirl burner (for the validation of combustion model).

2. Experimental setup

Experiments were carried out in the two swirl chambers, shown schematically in Fig. 1(a) and (b). The isothermal swirl chamber diameter (Fig. 1(a)), was 50 mm, and the height was 150 mm. The swirl flow was organized by a swirler (removable disc with 28 slots and with an inclination angle relative to the chamber axis). In the experiment with this chamber three swirlers were used with inclination angle 30°, 45° and 60° and three different swirl flow regimes were realized (with swirl numbers of 2.48, 1.7 and 0.85, respectively) where swirl number is defined as the ratio of angular momentum flux in axial direction and axial momentum flux in axial direction, Eq. (1).

$$S = \frac{2\pi \int Wr\rho Ur\,\mathrm{d}r}{2\pi R \int U\rho Ur\,\mathrm{d}r} \tag{1}$$

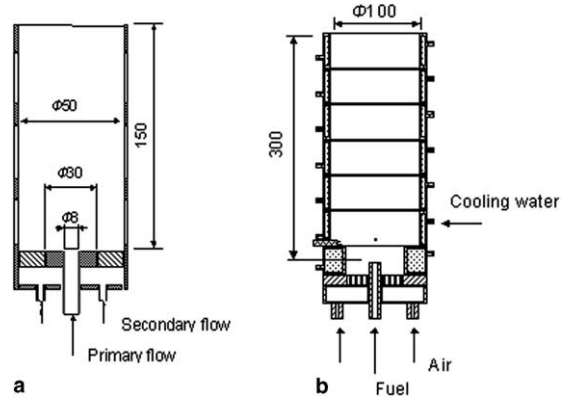

Fig. 1. Experimental swirl chambers, isothermal (a) and combustion chamber (b).

Velocity measurements have been carried out using one-component laser Doppler system. Instantaneous velocities in the axial and angular directions have been measured at the same point by rotating the LDA optics for 90°. All measurements have been carried out with a frequency shift of 5 MHz with long time stability of 10 e^{-7} Hz. An angle of 9° was chosen between the axis of the transmission optics and the axis of the receiver optics. With this optical arrangement dimensions of measuring control volume were $0.16 \times 0.16 \times 1.39$ mm. The primary and secondary flows were seeded with Al_2O_3 particles with a mean diameter of 2 μm.

The schematic presentation of the experimental combustion burner is given in Fig. 1(b). The experimental apparatus consisted of four basic parts: the experimental burner with the combustion chamber that consists of six

Table 1
The flow parameter for isothermal swirl chamber and combustion burner

Swirler angle φ [°]	Mass flow rate of primary flow $\dot{m}_p$ [kg/s]	Mass flow rate of secondary flow $\dot{m}_s$ [kg/s]	Swirl number S [–]
Isothermal swirl chamber			
30	4.473×10^{-5}	1.475×10^{-3}	0.85
45	4.467×10^{-5}	1.470×10^{-3}	1.7
60	4.465×10^{-5}	1.468×10^{-3}	2.48

	Mass flow rate of air $\dot{m}_a$ [kg/s]	Mass flow rate of fuel $\dot{m}_f$ [kg/s]	Swirl number S [–]	Surplus air α [–]
Combustion burner				
30	6.081×10^{-3}	2.099×10^{-4}	0.83	1.86
45	6.206×10^{-3}	2.300×10^{-4}	1.06	1.73
60	6.606×10^{-3}	2.663×10^{-4}	1.7	1.59

segments; a measurement and an acquisition equipment; a fuel and an air supplying line and the water cooling line. The swirl burner diameter was 100 mm, and the height was 300 mm.

The swirler in this case consisted of a removable disk with inclined plates, in which air annular flow gets tangential velocity component, and with an axial pipe for the introduction of fuel. Three swirlers, different in the inclination angels of slots (same as in the case of isothermal chamber) were used, providing three different swirling regimes with swirl numbers 0.83, 1.06 and 1.7. As a fuel, the equimolar ratio mixture of propane (C_3H_8) and butane (C_4H_{10}) was used. Between the swirler and the combustion chamber, Fig. 1(b), there exists s small space with diameter 18 mm and height 25 mm, in order to evade the sudden widening the secondary flow under the influence of centrifugal forces. The temperature and concentration measurements were carried out using the combined probe consisted of a thermocouple and a tube for gas sampling. Besides the temperature fields these experiments have provided data for CO_2 and O_2 concentration fields, for all three swirl regimes.

The flow parameter for isothermal swirl chamber and swirl burner are given in Table 1.

3. Mathematical model

3.1. Turbulent swirl flow modeling

In this paper a turbulent recirculating swirl flow is described by time-averaged Navier–Stokes equations and a k–ε model of turbulence for the determination of turbulent stress components. The effective viscosity hypothesis connects the Reynolds stresses to the mean velocity gradients. Reynolds stresses for the cylindrical, axisymmetrical flow arrangements can be expressed as follows:

$$-\rho\overline{uv}=\mu_t\left(\frac{\partial U}{\partial r}+\frac{\partial V}{\partial x}\right)$$

$$\begin{aligned}-\rho\overline{uw}&=\mu_t\frac{\partial W}{\partial x}\\ -\rho\overline{vw}&=\mu_t\frac{\partial}{\partial r}\left(\frac{W}{r}\right)\end{aligned}\qquad(2)$$

Turbulent and effective viscosities, according to k–ε model, are given by:

$$\mu_t=C_\mu\rho k^2/\varepsilon,\quad \mu_{\text{eff}}=\mu+\mu_t\qquad(3)$$

Obviously, to calculate Reynolds stresses the values of k and ε must be known. Those values are obtained from the solution of their respective transport equations [1].

Model of turbulent swirl flow, thus, consists of: mass conservation equation, momentum equations for velocities in axial (U), radial (V) and tangential (W) direction and transport equations for k and ε. All equations can be given in standard form for the conservation of a general variable Φ:

$$\begin{aligned}&\frac{\partial}{\partial x}(\rho U\phi)+\frac{1}{r}\frac{\partial}{\partial r}(r\rho V\phi)\\ &\quad=\frac{\partial}{\partial x}\left(\Gamma_{\text{eff}}\frac{\partial\phi}{\partial x}\right)+\frac{1}{r}\frac{\partial}{\partial r}\left(r\Gamma_{\text{eff}}\frac{\partial\phi}{\partial r}\right)+S_\phi\end{aligned}\qquad(4)$$

Dependent variables (Φ), diffusion coefficients (Γ_{eff}) and sources (S_Φ) for all conservation equations which describe the turbulent flow, as well as convective heat and mass transfer are listed in Table 2.

The swirl flow in a swirl chamber has complex 3D structure which complicates modeling of such class of flows. For the numerical analysis of the turbulent swirl flow, it is necessary to obtain the valid description of the rotation effect on the averaged and turbulent flow characteristics. The application range of existing approaches [2] using various modifications of the Richardson number is often limited.

For the validation of used turbulent mathematical model, experiments for three swirl regimes in this study had also been done.

Table 2
Dependent variables, diffusion coefficients and source terms in Eq. (4)

Equation	Dependent variable (ϕ)	Coefficient (Γ_{eff})	Source term (S_ϕ)
Continuity	1	0	0
Axial momentum	U	μ_{eff}	$\frac{\partial}{\partial x}\left(\mu_{\text{eff}}\frac{\partial U}{\partial x}\right)+\frac{1}{r}\frac{\partial}{\partial r}\left(\mu_{\text{eff}} r\frac{\partial V}{\partial x}\right)-\frac{\partial p}{\partial x}$
Radial momentum	V	μ_{eff}	$\frac{\partial}{\partial x}\left(\mu_{\text{eff}}\frac{\partial U}{\partial r}\right)+\frac{1}{r}\frac{\partial}{\partial r}\left(\mu_{\text{eff}} r\frac{\partial V}{\partial r}\right)-2\mu_{\text{eff}}\frac{V}{r^2}+\rho\frac{w^2}{r}-\frac{\partial p}{\partial r}$
Tangential momentum	W	μ_{eff}	$-\left(\frac{\mu_{\text{eff}}}{r^2}+\frac{\rho V}{r}+\frac{1}{r}\frac{\partial \mu_{\text{eff}}}{\partial r}\right)W$
Kinetic energy of turbulence	k	$\mu_{\text{eff}}/\sigma_k$	$G_{k_1}-\rho\varepsilon$
Dissipation of turbulence energy	ε	$\mu_{\text{eff}}/\sigma_\varepsilon$	$\frac{\varepsilon}{k}(C_1 G_{k_1}-C_2\rho\varepsilon)$
Stagnation enthalpy	h	$\mu_{\text{eff}}/\sigma_h$	S_R
Mass fraction of species k	m_k	$\mu_{\text{eff}}/\sigma_{\text{m}}$	$R_k(R_{\text{fu}})$

$$G_{k_1}=\mu_t\left\{2\left[\left(\frac{\partial U}{\partial x}\right)^2+\left(\frac{\partial V}{\partial r}\right)^2+\left(\frac{V}{r}\right)^2\right]+\left(\frac{\partial W}{\partial x}\right)^2+\left[r\frac{\partial}{\partial r}\left(\frac{W}{r}\right)\right]^2+\left(\frac{\partial U}{\partial r}+\frac{\partial V}{\partial x}\right)^2\right\}$$

Constants of model	C_μ	C_1	C_2	σ_k	σ_ε	σ_h	σ_{m}
Values	0.09	1.44	1.92	1.0	1.3	0.9	0.9

3.2. Heat transfer modeling

For determination of convective heat transfer it is necessary to solve the energy equation defined through the conservation of the gas stagnation enthalpy:

$$h=\sum_k m_k c_{p_k} T+\sum_k m_k H_{R_k}+\frac{1}{2}\left(U^2+V^2+W^2\right) \qquad (5)$$

where m_k denotes mass fractions of combustible components of the mixture and H_{R_k} their corresponding combustion heats. Energy equation can also be given in the form (4) where the source term represents radiation heat transfer (Table 2).

For the evaluation of radiative heat transfer the flux model of De Marco and Lockwood [3] was applied. This model showed good accuracy and computation economy and has been successfully used for the modeling of pulverized coal combustion.

When the six-flux model of De Marco and Lockwood is reduced to the axisymmetrical case, the equations for the mean radiation fluxes in axial (F_x) and radial (F_r) directions are:

$$\begin{aligned}&\frac{\partial}{\partial x}\left(\frac{1}{K_{\text{a}}}\frac{\partial F_x}{\partial x}\right)+K_{\text{a}}\left(-\frac{8}{3}F_x+\frac{4}{3}F_r+\frac{4}{3}E_{\text{B}}\right)=0\\&\frac{1}{r}\frac{\partial}{\partial r}\left(\frac{1}{K_{\text{a}}}r\frac{\partial F_r}{\partial r}\right)+K_{\text{a}}\left(-\frac{8}{3}F_r+\frac{4}{3}F_x+\frac{4}{3}E_{\text{B}}\right)=0\end{aligned} \qquad (6)$$

where K_{a} denotes the gas absorption coefficient and $E_{\text{B}}=\sigma T^4$ stands for the black body emissive power, with σ being the Boltzmann constant. Eq. (6) are coupled with the set of basic equations of the model (4), which describe the gas flow and convective heat and mass transfer through the coefficients in the Eq. (6) and the radiation source term S_R in the fluid stagnation enthalpy conservation equation. The expression for the radiation

source term was derived from the model of De Marco and Lockwood:

$$S_R = \frac{16}{9}K_a(F_x + F_r) - \frac{32}{9}K_a E_B. \quad (7)$$

The radiative heat transfer flux on the wall perpendicular to the x-direction is:

$$q_{wx} = 2\frac{\varepsilon_w}{2-\varepsilon_w}(E_{Bw} - F_{xw}) \quad (8)$$

where ε_w denotes the wall emissivity. The wall flux in the radial direction is determined by the expression analogous to (8).

It is important to note that radiation flux (6) has the same form as Eq. (4) which govern the fluid flow and convective heat and mass transfer, so that the same numerical method can be used for the solution of all combustion chamber model equations.

3.3. Convective mass transfer and combustion

The convective transfer of mass can be described by the conservation equations for the relevant components of the gas mixture, whose form corresponds to the standard form (4). Combustion model, proposed in this paper, is also based on the set of the conservation equations for the chemical species, where it is important to evaluate the source term that is determined by the combustion rate [4]. Proposed concept for the combustion modeling is appropriate for complex chemical reactions (consecutive, parallel, etc.) description. In this work, the two-step combustion approach was adopted.

The source terms in conservation equations for the chemical species of the two-step propane–butane mixture combustion are listed in Table 2. These source terms are given in dependence of rate of fuel conversion. Thus, the source terms evaluation in species conservation equations reduces to the combustion rate determination.

3.4. Combustion rate model

A proposed model of combustion rate is based on an eddy dissipation concept and k–ε model of turbulence, including simultaneous influence of chemical kinetics and turbulent mixing. Basic assumption of the model is that chemical reactions take place when reactants are mixed at molecular scale in isolated regions whose entire volume is a small fraction of the fluid elements. These regions are occupied by fine structures that represents end of cascade of eddy dissipation process, whose characteristic dimensions are of the same magnitude as the Kolmogorov micro-scale [5]. The probability contact of fluctuating reactants, essential in PDF modeling concept, was here substituted with the model of reactants

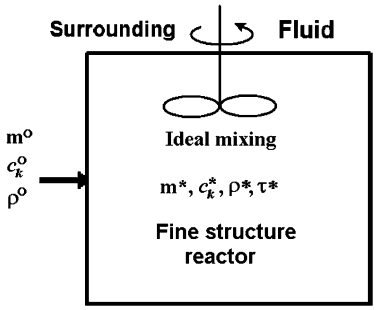

Fig. 2. Schematic illustration of the reacting zones.

mixing on molecular level inside the fine turbulent structures. Calculation of the overall combustion rate was thus reduced on the determination of the participation of fine structures in turbulence, and afterwards on the analysis of processes in fine structures. In the proposed model both the chemical kinetics and molecular mixing are considered at the same time, while in similar models [6,7] (EBU, C/D, etc.) the chemical kinetics was treated separately, or was neglected at all. Simultaneous influence of chemical kinetics and turbulent effects on the combustion rate is attained by treating fine structures like ideal chemical reactors, Fig. 2.

On the basis of the mass balance of species i in fine structures and surrounding fluid, and including the chemical kinetic rate, the conversion rate of species i can be expressed as:

$$R_i^* = \frac{c_i^\circ \frac{\rho^*}{\rho^\circ} - c_i^*}{\tau^*} = k_o e^{-\frac{E_a}{RT^*}} c_i^{*b_i} c_j^{*b_j} \quad (9)$$

where c_i^o and c_i^* are mass concentrations of species i, outside and inside the fine structures respectively:

$$m_i = c_i/\rho, \quad m_i^* = c_i^*/\rho^*, \quad m_i^\circ = c_i^\circ/\rho^\circ \quad (10)$$

Right side of Eq. (9) represents chemical reaction rate for the fine structure conditions, where k_o is the constant of chemical kinetics and b_i, b_j are order of chemical reaction rate.

Eq. (10) represents mass conversion rate of the species i within the existing life time of smallest eddies. It is equalised with the chemical kinetic rate for the fine structure conditions, analogously to ideal chemical reactors processes.

If the total mass m represents a sum of masses in fine structures m^* and surrounding m°: $m = m^* + m^\circ$, the mass fraction occupied by fine structures is defined as: $\gamma^* = m^*/m$. The relation between mean mass fraction and mass fraction for fine structure and surrounding fluid conditions of deficient species i in the particular control volume is given by:

$$m_k = (1-\gamma^*)m_k^\circ + \gamma^* m_k^* \quad (11)$$

Taking into account (10) and (11) the left side of the relation (9) takes the form:

$$R_i^* = \frac{\rho^*(m_i - m_i^*)}{\tau^*(1-\gamma^*)} \tag{12}$$

Eq. (12) represents conversion rate within reaction regions (fine structure).

Taking into account stoichiometric relation for chemical reaction, mass fraction of the second (over plus) reactant—j in the turbulent fine structures is defined by: $m_j^* = m_j^\circ - s_{j_i}(m_i^\circ - m_i^*)$, and applying (11) it can be expressed as:

$$m_j^* = m_j - s_{j_i}(m_i - m_i^*) \tag{13}$$

where $-s_{j_i} = (n_j M_j)/(n_i M_i)$ is stoichiometric ratio of the over plus j and deficient i species. Considering these relations the species i mass balance within the fine structure regions is:

$$\frac{\rho^*(m_i - m_i^*)}{\tau^*(1-\gamma^*)} = k_o \rho^{*(b_i+b_j)} \mathrm{e}^{-\frac{E_a}{RT^*}} m_i^{*b_i}[m_j - s_{j_i}(m_i - m_i^*)]^{b_j} \tag{14}$$

Now it is possible to calculate the combustion rate within the reaction regions (R_i^*) by using Eq. (12), but it is necessary to determine the variable m_i^*, by solving non-linear Eq. (14).

Reaction rate R_i^* for the deficient species (i) corresponds to the mass fraction occupied by fine structures. Taking this into account, total reaction rate in the case of the finite chemical reaction rate can be expressed by:

$$\begin{aligned} R_{\mathrm{fu}} &= R_i^* \gamma^* \quad \text{for } \frac{m_{ox}}{s_{\mathrm{fu}}} \geqslant m_{\mathrm{fu}} \quad \wedge \\ R_{\mathrm{fu}} &= \frac{R_i^* \gamma^*}{s_{\mathrm{fu}}} \quad \text{for } \frac{m_{ox}}{s_{\mathrm{fu}}} < y_{\mathrm{fu}} \end{aligned} \tag{15}$$

where $s_{\mathrm{fu}} = (n_{\mathrm{ox}} M_{\mathrm{ox}})/(n_{\mathrm{fu}} M_{\mathrm{fu}})$ is stoichiometric oxygen requirement.

As mentioned, the time scale for the fine structures corresponds to the Kolmogorov time scale:

$$\tau^* = a_\tau \sqrt{\nu/\varepsilon} \tag{16}$$

Mass fraction occupied by fine structures (γ^*) can be obtained as the ratio between Kolmogorov micro-scale and bulk mixing time scale: $\gamma^* = \tau^*/\tau_{\mathrm{m}}$. If we suppose that bulk mixing time scale is proportional to the turbulent macro-scale, the ratio of micro- and macro-scales τ^*/τ_{m} is proportional to $\sqrt{\nu/\varepsilon}/(l/\mathbf{u})$, where $\mathbf{u} = \sqrt{2/3k}$. and $\varepsilon = Au^3/l$. Therefore the mass fraction of the fine turbulent structures can be represented by the expression:

$$\gamma^* = a_\tau \frac{3a_\gamma}{2A} \sqrt{\frac{\nu\varepsilon}{k^2}}. \tag{17}$$

Taking into account that the fine structures, as well as the Kolmogorov micro-scale, are responsible for the dissipation of turbulent energy, it can be assumed that $a_\tau = 1$. Proposed values for constant A in the literature are among 0.1 and 1, but authors mainly recommend 0.6 [8]. Taking into account the results of EDC interstructural energy transfer modeling [5] it was assumed $a_\gamma = 0.18$.

Fluid density in fine structures was determined on the same way as for the mixture of ideal gases for conditions in reaction zones, using values of static pressure and temperature for surrounding fluid:

$$\rho^* = \frac{P}{RT^*}\left[\underbrace{\frac{m_i^*}{M_i}}_{\substack{\text{deficient}\\ \text{reagent}}} + \underbrace{\frac{m_j - s_{j_i}(m_i - m_i^*)}{M_j}}_{\text{reagent in excess}} + \underbrace{\sum_l \frac{m_l + s_{l_i}(m_i - m_i^*)}{M_l}}_{\text{combustion products}}\right]^{-1} \tag{18}$$

Combining Eqs. (12), (15)–(17) the combustion rate can be expressed as:

$$R_{\mathrm{fu}} = \begin{cases} \dfrac{C_{\mathrm{st}}\rho^*(m_i - m_i^*)}{\dfrac{2A}{3a_\gamma}\dfrac{k}{\varepsilon} - a_\tau\sqrt{\dfrac{\nu}{\varepsilon}}} & i = \mathrm{fu} \wedge C_{\mathrm{st}} = 1 \Rightarrow \dfrac{m_{\mathrm{ox}}}{s_{\mathrm{ox_{fu}}}} \geqslant m_{\mathrm{fu}} \\ & i = \mathrm{ox} \wedge C_{\mathrm{st}} = \dfrac{1}{s_{\mathrm{ox_{fu}}}} \Rightarrow \dfrac{m_{\mathrm{ox}}}{s_{\mathrm{ox_{fu}}}} < m_{\mathrm{fu}} \end{cases} \tag{19}$$

As mentioned before, in this work the two-step combustion, with carbon monoxide as intermediate was analyzed. The source terms in conservation equations for the chemical species of the two-step combustion are given (Table 2) in function of the fuel and carbon monoxide conversion rates ($R_{\mathrm{fu}}, R_{\mathrm{CO}}$). According to this the proposed combustion rate model based on ideal reactor analogy CO conversion rate can be determined by the expression:

$$R_{\mathrm{CO}} = k_{\circ_{\mathrm{CO}}} \rho^{*(b_{\mathrm{CO}}+b_{\mathrm{O_2}})} \mathrm{e}^{\frac{E a_{\mathrm{CO}}}{RT}} m_{\mathrm{CO}}^{*b_{\mathrm{CO}}} m_{\mathrm{O_2}}^{*b_{\mathrm{O_2}}} \gamma^* \tag{20}$$

The proposed submodel for the calculation of the combustion rate can be easily coupled with the other combustion chamber model equations, with the appropriate formulation of the source and sink terms in conservation equations for the reactants and products. Thus, reaction model parameters ($\tau^*, \gamma^*, \rho^*, m_i^*$), by which R_{fu}, and R_{CO} can be obtained, were calculated for each control volume.

The influence of the kinetic rate on total combustion rate is performed through the insufficient species (m_i^*) mass fraction in the combustion region (fine structures). The combustion rate, determined from (19) depends on temperature through m_i^*. That model property was illustrated on diagrams of Fig. 3.

The combustion rate can be also brought into the connection with the fluctuation characteristics that represent a result of the combustion and turbulence effects. It can be illustrated by comparison of Eq. (19) with the

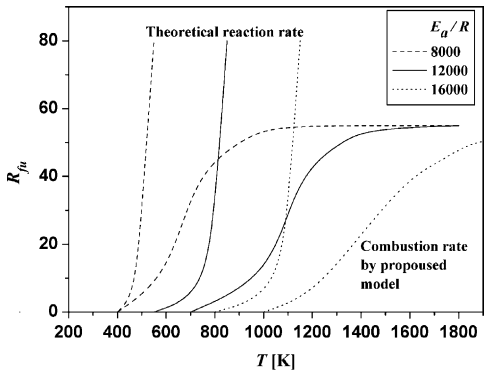

Fig. 3. Reaction rate temperature dependence.

corresponding equation of the advanced "eddy-break up" (EBU) model, of Spalding:

$$R_{\mathrm{EBU}} = \frac{\rho\sqrt{\overline{m_{\mathrm{fu}}'^2}}}{\frac{1}{C_{\mathrm{R}}}\frac{k}{\varepsilon}} \tag{21}$$

where m'_{fu} represents mass concentration fluctuations of fuel. Thus, we could assume the following relation: $m_i - m_i^* \approx \sqrt{\overline{m_i'^2}}$. Differences between Eqs. (19) and (21) in the denominators are the result of various turbulent combustion modeling approaches. EBU reaction rate modeling is based on consideration of the rate of break-up of the large eddies, while proposed model is based on chemical species balance within smallest eddies.

Numerical solution of the given system of equations has been obtained using the control volume method with iterative procedure of solution convergence [9]. Non-uniform numeric grid has been used in calculations.

4. Comparison of experimental and numerical results

The aim of this work is to analyze feasibility of the prediction of swirling reactive flow in cylindrical chamber, based on the comparison of the experimental results with the results obtained using mathematical model. Calculation results (model 1) were compared (beside with experimental data) with the version of model that comprises simplified proposed combustion rate model (model 2) and with the calculation that uses broadly applied version of EBU combustion rate model. In simplified version of the proposed model (model 2) the assumption that in combustion regions the kinetic rate is always infinitely fast ($m_i^* = 0$ and $\rho^* = \rho$) is implied. Hence, in this version it is not possible to take into account turbulent and kinetic effects simultaneously. Instead, the special criterion for determination of the minimum of chemical reaction kinetics rate and the turbulent diffusion rate was applied.

In this study validation of turbulent model has been done. The comparison of the measured and computed radial profiles of the mean velocity axial component and tangential component were presented in Figs. 4 and 5. Measured profiles of the mean velocity axial component and tangential component fit reasonably well with those obtained with computation. Computation shows that the recirculation zones are formed only in the regimes of flow with very high swirl ($S = 2.48$), which could be concluded from the experiments also. In the low swirl number regimes (0.85 and 1.7) the agreement of computation with experiments is especially good. This could be connected with the fact that the constants of standard k–ε model are adjusted for simulation of flows without swirl. As it has been already mentioned,

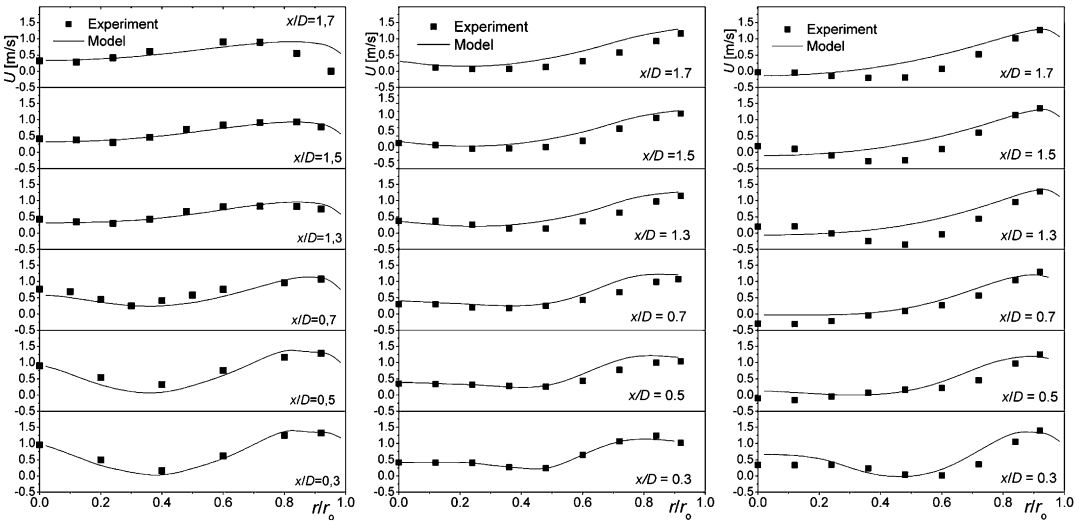

Fig. 4. Measured and calculated distributions of axial mean velocity U for isothermal chamber with different swirl numbers.

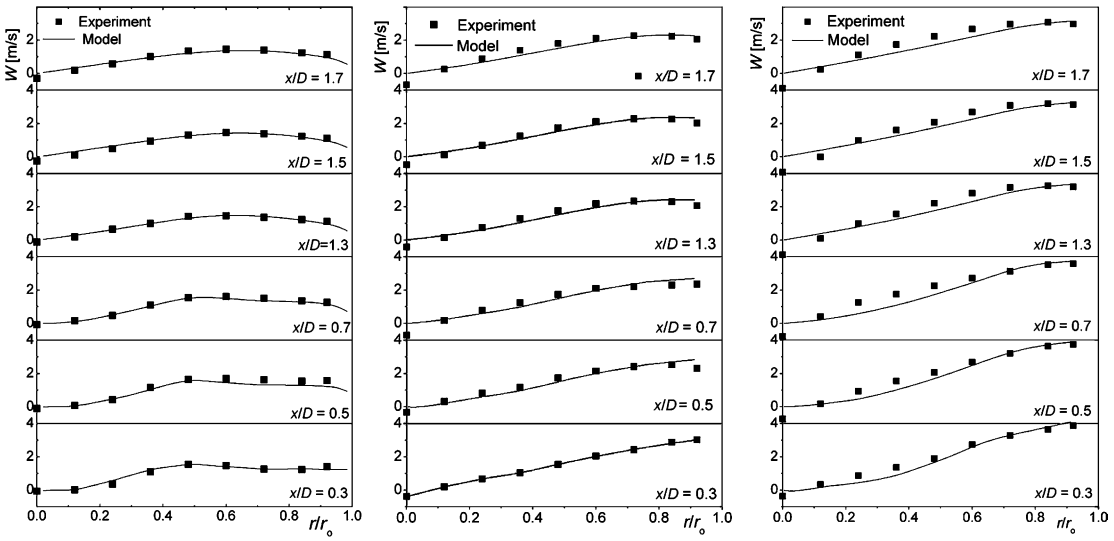

Fig. 5. Measured and calculated distributions of tangential velocity component W for isothermal chamber with different swirl numbers.

in these regimes there are no recirculation zones formed under the influence of swirl. The differences in computational and experimental results are visible on the diagrams which present flows with the most intensive swirl number ($S = 2.48$) especially in the regions with recirculation zones. Still, it can be concluded that there exists the satisfactory level of general agreement of computed profiles with those obtained in experiments. The axial position of recirculation zones in computation and measurements coincide ($x/D \approx 0.5$), but there are some difference in radial direction.

The noted disagreement in the value of mean velocities for regimes of the high swirl and close to the axes is probably the outcome of the lack of universality of the constants in k–ε model in the regions where centrifugal force is dominant, as well as of the anisotropic character of turbulent parameters of the considered flows. The more accurate computational results can be achieved with the extension of the computational domain on the viscous sublayer and with defining the constants of the k–ε model as functions of the turbulent Reynolds number, as well as with the use of the turbulent stress models.

$$R_{\mathrm{fu}} = \min\{R_{\mathrm{ch}}, R_{\mathrm{fu}}\} \tag{22}$$

In the applied version of the EBU model, instead of variance: $\sqrt{\overline{m'^2_{\mathrm{fu}}}}$ (20), mean mass fraction of fuel m_{fu} has been used. For taking into account a chemical kinetic effects a criterion (22) was applied.

Diagrams in Fig. 6 show the axial temperature profiles at five distances from chamber axis. Fig. 6 comprehends three flow cases with the following swirl numbers: $S = 0.83$, 1.06 and 1.7. As can be seen from these diagrams all three versions of proposed calculation show good agreement with the experimental results. However, some better agreement with the experimental results can be obtained by model 1. It is especially notable in regions near the gas inlet. The areas of significant dissimilarity between the calculations by model 2 and EBU model to experimental results and better agreement of the proposed model (model 1) corresponds to areas of bad combustion conditions (low temperatures, poor reactant mixing, etc.). Thus, proposed model provides better simulation characteristics for reacting flows where chemical kinetics and turbulent effects influence approximately equally the total reaction rate.

This difference between models 1 and 2 and EBU is possibly the result of the capability of simultaneous taking into account chemical kinetics and turbulent effects on total reaction rate in model 1, which is not the case in model 2 and EBU. In favor of this speaks the fact that there is only one common characteristic among models 2 and EBUmodel, and that is consideration of the chemical kinetics by separate criteria (22). On the other hand, there is only one difference between models 1 and 2, the way of consideration the influences of the chemical kinetics and turbulent effects on total reaction rate. Taking into account the same behavior of model 2 and EBU model it can be concluded that consideration of both the chemical kinetics and turbulent effects at the same time is crucial for these calculations. Both the experiments and model show that for more intensive swirl regimes these high temperature regions are placed closer to the burner and to the wall.

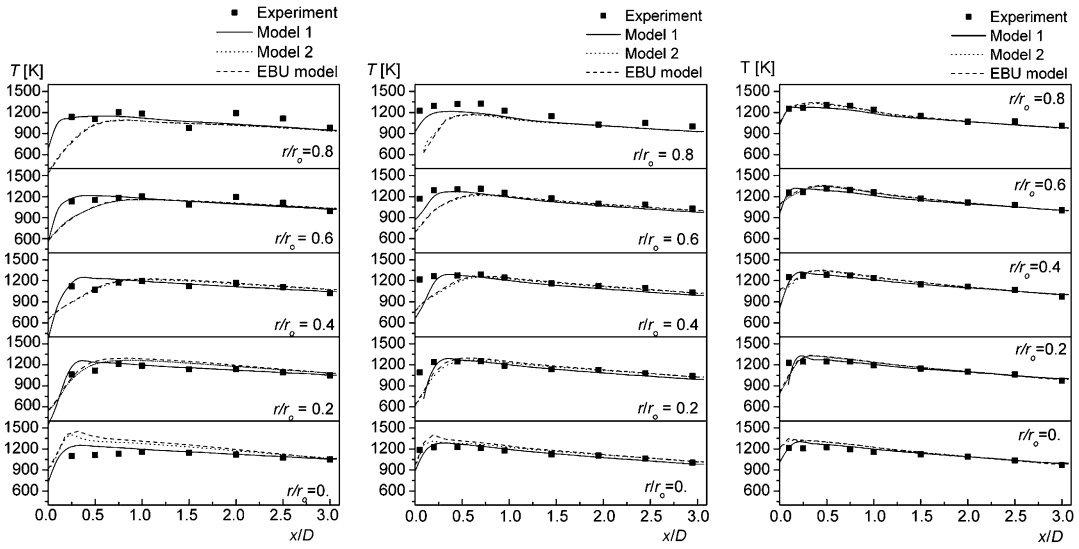

Fig. 6. Measured and calculated distributions of mean temperature for different swirl numbers.

Same conclusions can be obtained by comparative analysis of the results of measurement and calculation of the chemical species distribution. Figs. 7 and 8 show the axial CO_2 and O_2 concentration profiles respectively for dry combustion products, at five distances from chamber axis and for three different swirl regimes. In these figures it can also be seen the better agreement of model 1 then model 2 and EBU model with the experimental data, especially in intensive reaction zones.

Figs. 6–8 show good agreement of model 1 with experimental data. As can be seen in these figures the proposed model describes good the influence of the swirl intensity on combustion configurations. Flows with higher swirl number provide a smaller intensive combustion zones that are placed near the gas inlet regions. Thus, flow regimes with a more intensive swirl produce better reaction conditions and more combustion efficiency.

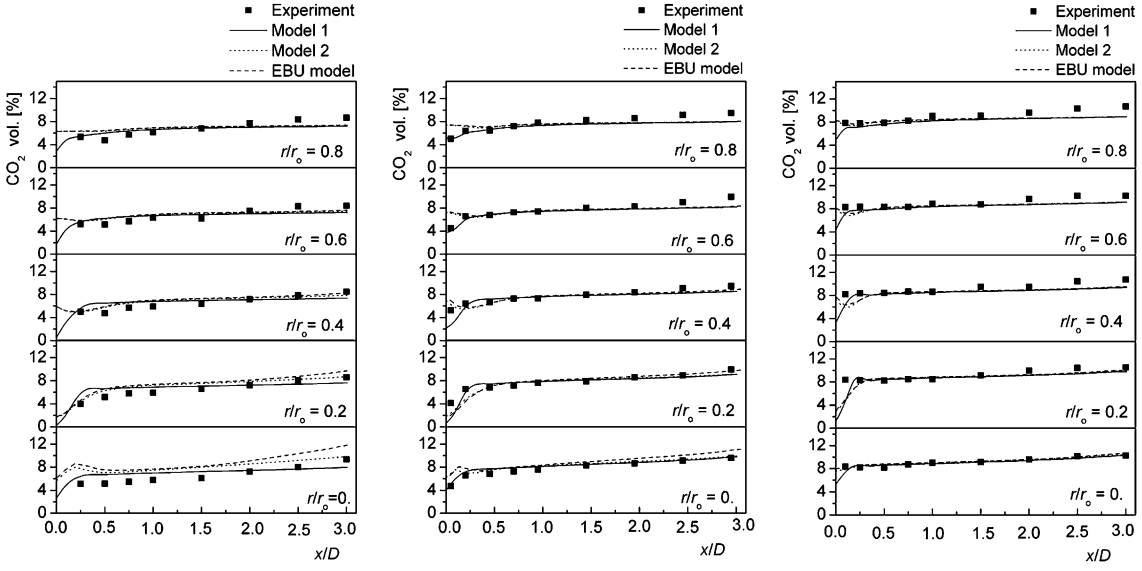

Fig. 7. Measured and calculated distributions of carbon dioxide concentration for different swirl numbers.

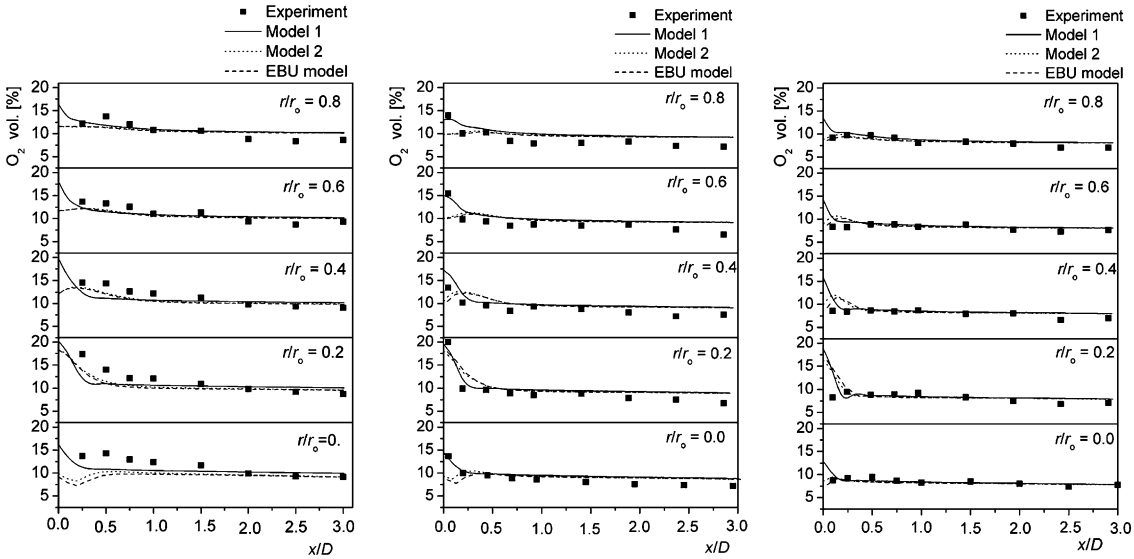

Fig. 8. Measured and calculated distributions of oxygen concentration for different swirl numbers.

5. Conclusions

The mathematical model for the prediction of gaseous fuel combustion processes was presented. It includes turbulent flow and convective heat and mass transfer segment, combustion segment and radiative heat transfer segment. It can be used as scientific and an engineering tool. Comparison of the measured temperature and concentration profiles with the calculation predictions shows good agreement of the proposed model with the experimental data. The basic advantage of the proposed numerical simulation procedure is application of the combustion model with EDC approach to calculation a combustion rate with simultaneous taking into account chemical kinetics and turbulent effects. The proposed model was applied on simulation of processes in water cooled combustion chamber with gas swirl flow, and calculation results were compared with experimental data. Beside experimental data the calculation results were compared with the version of model that comprises simplified combustion rate model and with the calculation that uses broadly applied version of EBU combustion rate model. The proposed simulation concept provides better simulation characteristic due to the possibility of simultaneous taking into account chemical kinetics and turbulent effects on total reaction rate. Model can also be applied on analysis of the influence of the flow regimes on combustion efficiency and temperature and concentration profile shapes in swirl combustion chamber.

References

[1] B.E. Launder, D.B. Spalding, The numerical computation of turbulent flows, Comput. Meth. Appl. Mech. Eng. 3 (1978) 269–289.

[2] D.G. Sloan, P.J. Smith, L.D. Smoot, Modeling of swirl in turbulent flow systems, Prog. Energy Combust. Sci. 12 (1986) 163–250.

[3] A.G. De Marco, F.C. Lockwood, A new flux model for the calculation of radiation in furnaces, La Rivista dei Combustibili 29 (1975) 184–204.

[4] S. Mahalingam, J.H. Chen, L. Vervisch, Finite-rate chemistry and transient effects in direct numerical simulations of turbulent nonpremixed flames, Combust. Flame 102 (3) (1995) 285–297.

[5] S. Byggstoyl, B.F. Magnussen, A model of flame extinction in turbulent flow, in: Proceedings of the Fourth Symposium on Turbulent Shear Flows, 1983, pp. 10.32–10.38.

[6] E.E. Khalil, D.B. Spalding, J.H. Whitelaw, The calculation of local flow properties in two dimensional furnaces, Int. J. Heat Mass Transfer 18 (1975) 775–791.

[7] E.E. Khalil, Modelling of Furnaces and Combustors, Abacus Press, Kent, 1982.

[8] R.J. Driscoll, L.A. Kennedy, A fluid element model for turbulent mixing and combustion, in: Proceedings of the 19th Symposium (International) on Combustion, 1982, pp. 387–392.

[9] S.V. Patankar, Numerical Heat Transfer and Fluid Flow, Hemisphere, New York, 1980.